Half-Metallic Digital Ferromagnetic Heterostructure Composed of a δ-Doped Layer of Mn in Si

M. C. Qian,[1,*] C. Y. Fong,[1] Kai Liu,[1] W. E. Pickett,[1] J. E. Pask,[2] and L. H. Yang[2]

[1]*Department of Physics, University of California, Davis, Davis, California 95616-8677, USA*

[2]*Lawrence Livermore National Laboratory, University of California, Livermore, California 94551, USA*

(Received 31 July 2005; published 19 January 2006)

We propose and investigate the properties of a digital ferromagnetic heterostructure consisting of a δ-doped layer of Mn in Si, using *ab initio* electronic-structure methods. We find that (i) ferromagnetic order of the Mn layer is energetically favorable relative to antiferromagnetic, and (ii) the heterostructure is a two-dimensional half-metallic system. The metallic behavior is contributed by three majority-spin bands originating from hybridized Mn-d and nearest-neighbor Si-p states, and the corresponding carriers are responsible for the ferromagnetic order in the Mn layer. The minority-spin channel has a calculated semiconducting gap of 0.25 eV. The band lineup is found to be favorable for retaining the half-metal character to near the Curie temperature. This kind of heterostructure may be of special interest for integration into mature Si technologies for spintronic applications.

Doping magnetic transition metal elements into semiconductors has attracted much attention recently, especially the doping of Mn in GaAs [1], which has inspired much interest in the new and immensely promising field of spintronics [2–4]. Since 2000, a new class of potential spintronic materials has been discovered: the half-metallic transition metal pnictides with zinc blende structure. Two such compounds, CrAs [5] and CrSb [6], have been grown in thin film form. Many other pnictides and carbides [7–9] have been predicted based on first-principles calculations in the generalized gradient approximation (GGA) [10]. Related quantum structures, such as superlattices [11–13] and quantum dots [14], have also been studied. Sanvito and Hill [15] investigated the half-metallic properties of a digital ferromagnetic heterostructure (DFH) composed of a layer of Mn in GaAs. The key property of all such half-metallic materials is the 100% spin polarization at the Fermi energy, E_F. Therefore, the magnetoresistance (MR) effect is expected to be much larger and becomes infinite in the ideal case. Devices made of these materials, such as MR sensors, memories, and switches, will have superior qualities to the ones presently available. However, the realization of devices based on these materials has been hindered by difficulties in growth and fabrication processes involving III-V compounds. Fabrication techniques for Si based devices are more mature; and so they might be more readily manufactured, if corresponding half-metallic devices could be engineered. The prediction of ferromagnetic order in Mn-doped bulk Si [16] and the growth of dilutely doped Mn in Si [17,18] have been reported. The experimental results are particularly encouraging because the measured Curie temperature, T_C, is over 400 K, in stark contrast to Mn-doped GaAs which suffers from a T_C far below room temperature. A critical shortcoming of Mn-doped GaAs with respect to spintronic applications might thus be surmounted by such Si based materials.

Here, we report our design of a DFH consisting of a δ-doped layer of Mn in a Si substrate (Mn/Si-DFH), with a δ function (single layer) doping profile along the growth direction, and our prediction that this DFH is a two-dimensional half-metal. We find that the metallic properties are contributed by extended states originating from hybridized Mn-d and nearest-neighbor Si-p majority-spin states, while the minority-spin channel is semiconducting with a 0.25 eV gap.

We employed plane wave pseudopotential density-functional methods [19], in the GGA to exchange and correlation [10]. Ultrasoft pseudopotentials [20] were used to facilitate the accurate treatment of transition metal atoms. The heterostructure was modeled by a unit cell consisting of 32 atoms in layers along the [001] direction of epitaxial growth, as shown in Fig. 1. The unit cell is tetragonal with **a** and **b** axes along the [110] and [$\bar{1}$10] directions, and lattice constant $a_0/\sqrt{2}$, where $a_0 = 5.45$ Å is the optimized lattice constant of Si crystal. The indices are defined with respect to the conventional cell. We have checked the effect of the thickness of the Si region from 15 to 39 Si layers along the [001] direction. The half-metallic properties and the density states of the majority spin at E_F remain unaffected. The gap between the lowest unoccupied state in the minority-spin channel and E_F is 0.15 eV at 15 Si layers separation and stabilized to 0.16 eV at separations of 31 Si layers or more. Further details will be presented elsewhere [21]. The separation between Mn layers in neighboring cells was sufficient to make cell-cell interactions negligible, as we discuss below. A plane wave cutoff of 450 eV and Monkhorst-Pack [22] mesh of $11 \times 11 \times 1$ **k** points was used in all calculations. Larger **k**-point sets were employed to verify convergence of the above set to the order of 1 meV/atom. Wigner-Seitz sphere radii of 1.35 Å and 1.32 Å were used for Mn and Si atoms, respectively, to construct projected densities of states.
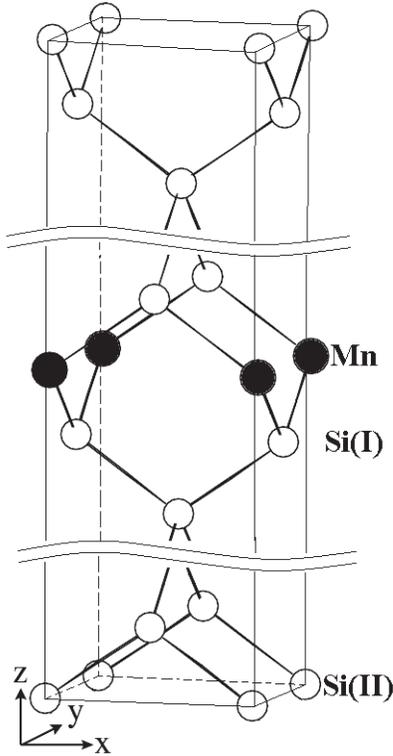
FIG. 1.   Mn/Si-DFH unit cell, consisting of 32 layers in the z direction. Black circles denote Mn; open circles denote Si.

Atomic positions were optimized by conjugate-gradient minimization of the total energy.

The magnetic moment per unit cell, density of states at the Fermi energy, and energy difference between ferromagnetic and antiferromagnetic ordering for the unrelaxed and relaxed cases are given in Table I. Without lattice relaxation, the magnetic moment is an integer, $3.0\mu_B$. There is a gap of 0.20 eV in the minority-spin states. The effect of lattice relaxation is small because the optimized lattice constant of Si (5.45 Å) is close to that of (hypothetical) zinc blende MnSi (5.48 Å) [21]. The gap for the relaxed case opens slightly to 0.25 eV. Both with and without relaxation, the ferromagnetic phase has lower energy than the antiferromagnetic phase. Since the relaxation effect will not alter our conclusions about DFH, in the following, we focus our analysis on the unrelaxed case.

The total and partial densities of states (PDOS) for the majority- and minority-spin channels are shown in Fig. 2. The PDOSs show projections onto the Mn, nearest Si [Si(I)], and farthest Si [Si(II)] atoms. Considering first the majority-spin states, we find a finite density of states at E_F, as shown in the top panel. The states in a 3 eV range around E_F (from ~ -1 to $+2$ eV) show strong hybridization between Mn-t_{2g} and Si(I)-p states (second and third panels). In contrast, there is no significant contribution from the more distant Si(II) atoms. The bonding states centered ~ 2.6 eV below E_F exhibit correspondingly strong Mn-t_{2g}-Si(I)-p character. The nonbonding Mn-e_g

TABLE I.   Comparison of the unrelaxed and relaxed cases for Mn δ-doped in Si. The magnetic moment m, density of states at the Fermi energy $N(E_F)$ per eV-unit cell, ferromagnetic-antiferromagnetic energy difference $E_{FA} = E_{FM} - E_{AFM}$, and minority-state gap E_g are listed. The difference E_{FA} is calculated for the unit cell with one Mn-Mn pair. For both cases, the ferromagnetic ordering has lower energy.

	$m(\mu_B)$	$N(E_F)$	E_{FA} (meV)	E_g (eV)
Unrelaxed	3.0	1.06	-523.91	0.20
Relaxed	3.0	1.25	-442.38	0.25

states are located ~ 2.5 eV below E_F, concentrated in a somewhat narrower range of about 1 eV. The conduction states ~ 2 eV above E_F and higher are contributed mainly by the Si atoms. Considering now the minority-spin channel, we find a semiconducting gap of ~ 0.20 eV between valence and conduction bands. The valence states are mainly bulk Si, with one band of Mn-t_{2g}-Si(I)-p character at ~ 1 eV below E_F. The conduction states originate from both antibonding p-t_{2g} hybrid states and nonbonding e_g states of the Mn, leading to a peak at ~ 0.5 eV. The more distant Si(II) atoms contribute a broad manifold extending to 4 eV below E_F, much as in Si crystal. The results indicate that the interaction of the Mn atom is confined primarily to its nearest-neighbor Si(I) atoms.

The band structure along symmetry lines in the $\mathbf{k}_x$-$\mathbf{k}_y$ plane (Γ-R-X-Γ) and along the $\mathbf{k}_z$ direction (Γ-Z) in the
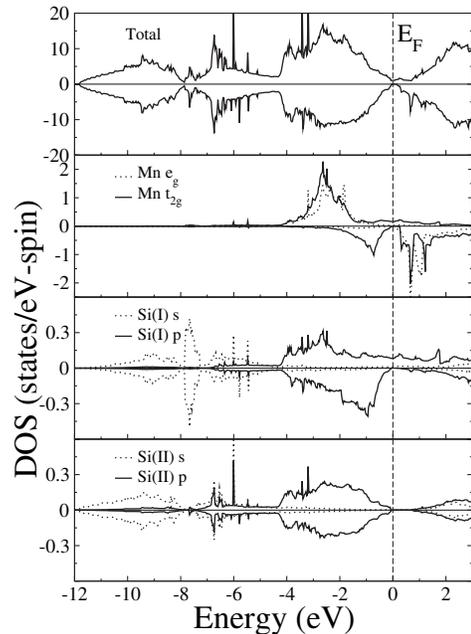

FIG. 2.   Calculated total and partial densities of states for Mn δ-doped in Si. Si(I) and Si(II) refer to nearest and farthest silicons from Mn. Majority densities are plotted as positive values; minority densities as negative. The vertical dashed line indicates the Fermi energy.

energy range -1.5 to 1.5 eV is shown in Fig. 3. The sizes of the circles indicate the contribution from Mn-d states: larger circles indicate larger contributions. In Fig. 3(a), three majority-spin bands pass through the Fermi energy in the $\mathbf{k}_x$-$\mathbf{k}_y$ plane. We label these bands 1, 2, and 3. The lowest energy states of the three bands are at the R point and are occupied. Around the Γ point, the three bands are unoccupied. As discussed above in PDOS, the states in the vicinity of E_F contributing to the conduction originate from the hybridization of Mn-t_{2g} and (near-neighbor) Si(I)-p states. Along Γ-Z, the marked flatness of the associated bands indicates the negligible interaction between Mn planes: the states are extended along the planes and well localized perpendicular to them, forming a metallic two-dimensional sheet of majority carriers only. Compared to the corresponding bands along Γ-X of the Mn/GaAs DFH studied by Sanvito and Hill [15], the partially filled bands in Mn/Si-DFH are substantially broader, reflecting the more ionic character of the As atoms relative to Si. In Fig. 3(b), the band structure for the minority-spin channel is shown. The semiconducting gap is indirect with the top of the valence band near the Γ point and the bottom of the conduction band at the zone corner R point. From the above, then, it is clear that the carriers in the Mn/Si-DFH come from three majority-spin bands, and mediate the exchange interactions between the local magnetic moments which give rise to the ferromagnetic order in the Mn layer. The band structures given in Figs. 3(a) and 3(b)
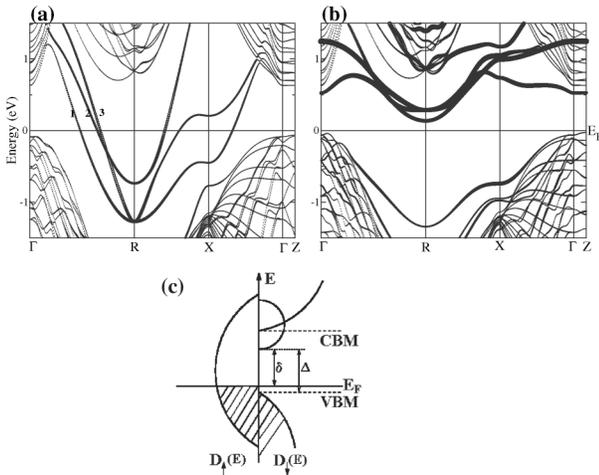
exhibit clearly the marked two-dimensional half-metallic character of the heterostructure.

In order to better characterize the relevant conduction states, we examine the Fermi surfaces and associated charge density in Fig. 4. The band 1 forms a hole pocket, a surface with closed orbit, around the Γ point. Bands 2 and 3 form two electron surfaces centered at the R point in the $\mathbf{k}_x$-$\mathbf{k}_y$ plane. In Fig. 4(b), as an example for illustration, the corresponding majority-spin hole charge densities are obtained by integrating states in the vicinity of E_F up to 0.5 eV. It can be seen that the hole states are strongly confined in the vicinity of the Mn layer and distributed in the bonding directions between Mn and Si(I) atoms.

One important question is whether the half-metallic character can be maintained up to T_C in this DFH. Based on an analysis of available experimental data on NiMnSb alloys, Hordequin et al. [23] identified the temperature T^* (80 K) well below T_C (730 K) at which NiMnSb undergoes an electronic phase transition from half-metal to normal ferromagnet. This crossover occurs because the minority band gap is the result of exchange splitting of bands, which is proportional to the magnetization and decreases as temperatures increase. The interpretation is that one of the gap edges crosses the Fermi level as the gap decreases, thereby losing the half-metal character. From Hall measurements, they found that the hole concentration increases with temperature and that the low T^* is the signature of spin-flip transitions from the majority-spin states at E_F to the bottom of the conduction band of the minority-spin channel, which become allowed as the gap decreases. They concluded that T^* could reach T_C if E_F lies near the top of the valence band of the minority-spin channel, rather than near the bottom of the conduction band. Unlike NiMnSb, this advantageous band lineup does occur in the band structure of Mn/Si-DFH shown in Fig. 3. Figure 3(c) shows a schematic diagram of density of states of Mn/Si-DFH near the E_F. The spin-flip gap δ between the Fermi energy and the bottom of the conduction band in the minority-spin channel is about 0.16 eV, which is close to the semiconducting gap $\Delta = 0.20$ eV from the valence band maximum
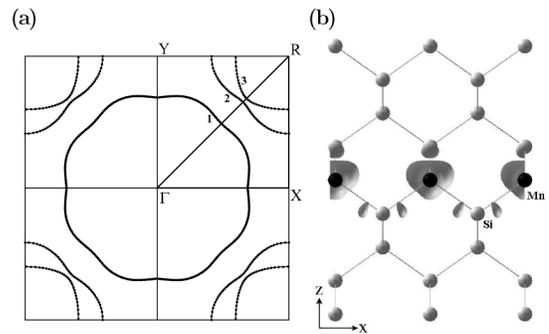

FIG. 3. Calculated band structure along Γ-R-X-Γ in the $\mathbf{k}_x$-$\mathbf{k}_y$ plane and along Γ-Z in the $\mathbf{k}_z$ direction, (a) spin-up and (b) spin-down for Mn δ-doped in Si. High symmetry points of the Brillouin zone are $\Gamma = (0, 0, 0)$, $R = (1, 1, 0)$, $X = (1, 0, 0)$, and $Z = (0, 0, 1)$. The size of circles indicates the fraction of Mn d character. The conduction bands are labeled 1, 2, and 3. (c) Schematic diagram of the density of states $D(E)$ in Mn/Si-DFH of the two spin channels near E_F. VBM and CBM are the valence band maximum and conduction band minimum, respectively, of Si crystal for comparison.

FIG. 4. (a) Calculated two-dimensional Fermi surfaces. (b) Majority-spin hole charge density in the vicinity of E_F for Mn δ-doped in Si.

to the bottom of the conduction band in the minority-spin channel. In addition, the bottom of the conduction band is well below the conduction band minimum of host Si crystal. At finite temperature, there are two possible spin-flip transitions due to the interaction between the spin of a carrier and the fluctuation of local moments of the Mn atoms. One is the transition from the top of valence states in the minority-spin channel to the majority states at E_F, but this will be strongly suppressed by matrix element effects because the uppermost valence states are bulk Si bonding states whereas the states at E_F are Mn-d Si(I)-p hybridized and they only weakly overlap bulk Si states. Thus, as in NiMnSb, only the second one dominates the spin-flip scattering and deteriorates the half-metallicity, because both the majority states at E_F and the minority states at the bottom of conduction band are coming from the hybridized Mn d-Si p states. This second process, of an electron at the E_F undergoing a spin-flip transition to the bottom of conduction band, involves the so-called spin-flip gap δ. It should be mentioned that the GGA usually underestimate the semiconducting gap of Si crystal, and a wider gap δ should be more realistic. Therefore, for the Mn/Si-DFH, the half-metallic character could persist up to a temperature comparable to T_C.

In summary, using first-principles electronic-structure methods, we have designed a low strain DFH composed of a Mn δ-doped layer in Si substrate, which exhibits two-dimensional half-metallic properties. The metallic states are hybrid states originating from Mn-t_{2g} and nearest-neighbor Si-p states in the majority-spin channel. A semi-conducting gap is retained between minority-spin bonding and antibonding states. From the DOS and band structure, the half-metallic properties are shown to have marked two-dimensional character and are likely to persist up to $T^* \approx T_C$, in marked contrast to NiMnSb.

Since the measured T_C in dilutely doped Mn in bulk Si is approximately 400 K [17,18], the T_C for this ordered DFH may be substantially higher than room temperature. Because of the maturity of Si technologies, it may be expected that Si based devices will be more readily fabricated than their GaAs based counterparts. If the designed DFH can be grown, such Si based half-metallic materials could lead to a breakthrough in the realization of spintronic devices in the near future, and to a new generation of devices in the years to come.

*Electronic address: mqian@physics.ucdavis.edu

[1] Y. Ohno, D. K. Young, B. Beschoten, F. Matshkura, H. Ohno, and D. D. Awschalom, Nature (London) **402**, 790 (1999).
[2] G. A. Prinz, Science **282**, 1660 (1998).
[3] P. Ball, Nature (London) **404**, 918 (2000).
[4] W. E. Pickett and J. S. Moodera, Phys. Today **54**, No. 5, 39 (2001).
[5] H. Akinaga, T. Manago, and M. Shirai, Jpn. J. Appl. Phys. **39**, L1118 (2000).
[6] J. H. Zhao, F. Matsukura, T. Takamura, E. Abe, D. Chiba, and H. Ohno, Appl. Phys. Lett. **79**, 2776 (2001).
[7] J. E. Pask, L. H. Yang, C. Y. Fong, W. E. Pickett, and S. Dag, Phys. Rev. B **67**, 224420 (2003).
[8] I. Galanakis and P. Mavropoulos, Phys. Rev. B **67**, 104417 (2003).
[9] W.-H. Xie, Y.-Q. Xu, and B.-G. Liu, Phys. Rev. Lett. **91**, 037204 (2003).
[10] J. P. Perdew, K. Burke, and M. Ernzerhof, Phys. Rev. Lett. **77**, 3865 (1996).
[11] C. Y. Fong, M. C. Qian, L. H. Yang, J. E. Pask, and S. Dag, Appl. Phys. Lett. **84**, 239 (2004).
[12] C. Y. Fong and M. C. Qian, J. Phys. Condens. Matter **16**, S5669 (2004).
[13] M. C. Qian, C. Y. Fong, W. E. Pickett, J. E. Pask, L. H. Yang, and S. Dag, Phys. Rev. B **71**, 012414 (2005).
[14] M. C. Qian, C. Y. Fong, W. E. Pickett, and Huai-Yu Wang, J. Appl. Phys. **95**, 7459 (2004).
[15] S. Sanvito and N. A. Hill, Phys. Rev. Lett. **87**, 267202 (2001).
[16] H. Weng and J. Dong, Phys. Rev. B **71**, 035201 (2005).
[17] M. Bolduc, C. Awo-Affouda, A. Stollenwerk, M. B. Huang, F. G. Ramos, G. Agnello, and V. P. LaBella, Phys. Rev. B **71**, 033302 (2005).
[18] F. M. Zhang, X. C. Liu, J. Gao, X. S. Wu, Y. W. Du, H. Zhu, J. Q. Xiao, and P. Chen, Appl. Phys. Lett. **85**, 786 (2004).
[19] G. Kresse and J. Hafner, J. Phys. Condens. Matter **6**, 8245 (1994); G. Kresse and J. Furthmuller, Phys. Rev. B **54**, 11 169 (1996).
[20] D. Vanderbilt, Phys. Rev. B **41**, R7892 (1990).
[21] M. C. Qian *et al.* (to be published).
[22] H. J. Monkhorst and J. D. Pack, Phys. Rev. B **13**, 5188 (1976).
[23] C. Hordequin, D. Ristoiu, L. Ranno, and J. Pierre, Eur. Phys. J. B **16**, 287 (2000).